Machine Learning for Disseminating Cooperative Awareness Messages in Cellular V2V Communications

Journal:	*IEEE Transactions on Vehicular Technology*
Manuscript ID	VT-2021-03221
Suggested Category:	Regular Paper
Date Submitted by the Author:	09-Sep-2021
Complete List of Authors:	Lusvarghi, Luca; University of Modena and Reggio Emilia, Department of Engineering "Enzo Ferrari" Merani, Maria Luisa; University of Modena and Reggio Emilia, Department of Engineering "Enzo Ferrari"
Keywords:	Vehicular Communications, NR-V2X, C-V2X, Wireless Intelligence

Machine Learning for Disseminating Cooperative Awareness Messages in Cellular V2V Communications

Luca Lusvarghi, *Graduate Student Member, IEEE* and Maria Luisa Merani, *Senior Member, IEEE*

***Abstract*—This paper develops a novel Machine Learning (ML)-based strategy to distribute aperiodic Cooperative Awareness Messages (CAMs) through cellular Vehicle-to-Vehicle (V2V) communications. According to it, an ML algorithm is employed by each vehicle to forecast its future CAM generation times; then, the vehicle autonomously selects the radio resources for message broadcasting on the basis of the forecast provided by the algorithm. This action is combined with a wise analysis of the radio resources available for transmission, that identifies subchannels where collisions might occur, to avoid selecting them. Extensive simulations show that the accuracy in the prediction of the CAMs' temporal pattern is excellent. Exploiting this knowledge in the strategy for radio resource assignment, and carefully identifying idle resources, allows to outperform the legacy LTE-V2X Mode 4 in all respects.**

***Index Terms*—LTE-V2X, Vehicular Machine Learning, CAM, safety messages, wireless intelligence.**

I. Introduction and State of the Art

Present days witness an increased and widespread sensitivity to road safety and sustainable transports. Day 1 safety applications are already present on vehicles, to increase space awareness and grant the car and its driver more time to react to unexpected situations. Safety will be further improved by upcoming applications, whose distinctive feature is to rely on vehicular communications. The onset of vehicular networking represents a major turning point, as it lies the basis for Day N services, where fully autonomous and cooperative driving turn into reality, and the goal of secure and more environment-friendly transports is accomplished.

In the field of vehicular communications, Long Term Evolution Vehicle-to-Everything (LTE-V2X) is the current cellular standard, and Mode 4 represents the baseline approach for safety services, as its communications occur with no network assistance The performance of Mode 4 distributed radio resource selection and scheduling has been investigated by numerous works [1]–[6]. Recently, some investigations outlined that LTE-V2X falls short when dealing with aperiodic, unpredictable packet flows [7] [8], and also struggles when transmitting aperiodic messages of variable size [10]. New Radio (NR)-V2X, the LTE-V2X evolution in the fifth generation (5G) of cellular networks, inherits the majority of LTE-V2X core choices and, as a consequence, the question of how to schedule aperiodic traffic remains unanswered.

The current work intends to offer a contribution in this domain, taking a fresh look at the problem of aperiodic safety message dissemination. It concentrates on the main traffic type that LTE-V2X was designed to deliver, namely, Cooperative Awareness Messages (CAMs), application-layer packets standardized by the European Telecommunications Standards Institute (ETSI), and it proposes to harness Machine Learning (ML) to effectively broadcast such messages.

As matter of fact, ML has recently stirred an unprecedented interest and consensus in numerous wireless settings. This major branch of artificial intelligence is often seen as the appropriate tool to pick the lock of complex problems encountered in, e.g., radio resource allocation and optimization; with no ambition for completeness, [11]–[13] represent captivating examples in the field. The survey in [14] offers an excellent portray of the recent ML applications to the specific domain of vehicular networks. However, to the authors' knowledge, none of the studies in the field have scouted the adoption of ML in V2V safety communications.

This study proposes to interpret the aperiodic CAM sequence as a series of sub-sequences that are periodic over a short time scale, and to rely on ML to forecast the sub-sequence length and periodicity. Then, the idea is to tailor LTE-V2X radio resource reservations so as to fit the period and length of the single sub-sequence forecast by ML, reducing the risk of future collisions. Additionally, the identification of free radio resources performed by LTE-V2X (and NR-V2X) is modified and made more effective. The main outcomes of this work are as follows:

- ML achieves an excellent accuracy in predicting the temporal patterns of CAMs;
- the new, ML-enhanced scheduling of resources outperforms LTE-V2X Mode 4 under all points of view, warranting higher rates of packet delivery, fewer collisions and better channel utilization.

When the literature on CAM distribution is explored, it is worth recalling [15], which determined an accurate broadcasting threshold and broadcasting interval, as well as [16], that proposed a novel triggering condition based on the road radius, assumed as a risk indicator. Moreover, the authors of [17] explored a simple mechanism to confine the queueing delays suffered by CAMs when they coexist with different traffic types. In the above-referenced papers, the authors intervened beforehand, modifying the generation pattern of CAM traffic.

The authors are with the Department of Engineering "Enzo Ferrari", University of Modena and Reggio Emilia, Modena 41125, Italy (e-mail: luca.lusvarghi5@unimore.it; marialuisa.merani@unimore.it) and also with Consorzio Nazionale Interuniversitario per le Telecomunicazioni, CNIT.

Manuscript received XXX, XX, 2015; revised XXX, XX, 2015.

As opposed to such contributions, the current work forecasts when next CAMs will be generated in accordance with the ETSI EN 302 637-2 standard [18] and reserves resources accordingly, modifying the LTE-V2X scheduling in a very effective manner.

An alternative approach was taken in [19], where CAMs were compressed to reduce the channel load, and in [20], where the LTE-V2X resource allocation was tuned to the different sizes that data packets exhibit. In the last two references, the issue of radio resource assignment was considered; yet, in the former contribution, the authors themselves evidenced that compressing and decompressing is time consuming; as regards the last paper, it is observed that the size of CAM messages is not known *a priori* and can vastly vary, which prohibits an effective adoption of the second solution. On a different rim, both [21] and [22] considered message delivery for cooperative awareness, but focused on Carrier Sense Multiple Access/Collision Avoidance (CSMA/CA), the access strategy adopted in the Medium Access Control (MAC) sublayer of 802.11p. Namely, [21] considered a simplified, periodic model for CAM traffic and leveraged on full-duplex transceivers; [22] highlighted the impact of realistic mobility patterns on the 802.11p operation. On the contrary, our contribution is centered on LTE-V2X, the competitor standard; it is the latter that represents the actual term of comparison when assessing the behavior of the newly proposed, ML-based scheduling scheme.

Additional references are represented by [23] through [26]: the authors of [23] examined LTE-V2X Mode 3, hence the scenario where the eNodeB controls the allocation of resources to V2V communications; the authors of [24] investigated a centralized multicast/broadcast approach too. Conversely, our solution is totally decentralized, as LTE-V2X Mode 4 mandates. The study in [25] faced the design of V2V communications and employed the sub-6 GHz band exclusively for the control plane, whereas the data plane was positioned at mmWave frequencies. Similarly to [25], [26] considered mmWave communications and allowed for multi-hop transmissions among vehicles. On the contrary, the current investigation is sub-6 GHz centered and examines single-hop transmissions, adhering to the standard guidelines for cellular vehicular communications. Within this framework, [7] and [8] already highlighted how the non-ideal periodicity of packet generation affects the operation and performance of C-V2X in LTE; 5G vehicular communications were studied in [9] and similar conclusions were drawn with reference to aperiodic traffic. Here, our former studies are continued and a new research path is paved, as:

- it is asked whether ML can help in serving aperiodic traffic in LTE-V2X, given the latter is a recognized benchmark for safety communications in a vehicular environment;
- a largely positive answer is provided. The LTE-V2X standard is therefore enhanced with a mechanism to predict when CAMs will be generated and when to reserve radio resources on the time-frequency grid of LTE.

The rest of the paper is organized as follows. In Section II, the main features of LTE-V2X are recalled, along with the challenges that the standard Mode 4 faces in the dissemination of aperiodic traffic. The generation rules of CAMs and their intrinsic aperiodicity are also discussed. In Section III, the ML-based policy to accommodate aperiodic CAM traffic on the time-frequency grid that LTE-V2X adopts is presented in detail. In Section IV, the metrics to evaluate the performance of any radio resource assignment strategy in a vehicular environment are introduced. In Section V, the simulation results are presented and the conclusions are drawn in Section VI.

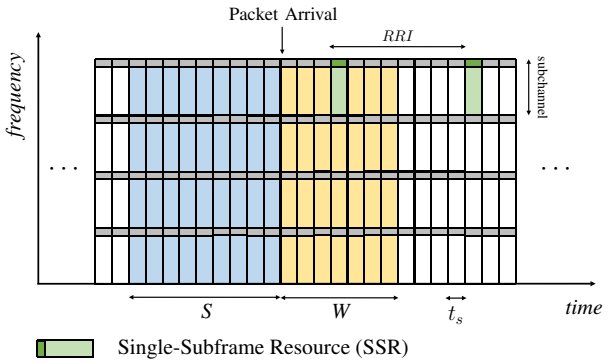

Fig. 1. LTE-V2X time-frequency resource grid

II. C-V2X Communications

A. LTE-V2X in Release 14

The LTE-V2X solution for vehicular communications has been standardized by the Third Generation Partnership Project (3GPP) in Release 14. Also known as Cellular Vehicle-to-Everything (C-V2X), this technology was mainly designed to disseminate CAMs, Decentralized Environmental Notification Messages (DENMs) and Basic Safety Messages (BSMs), and therefore to allow the development of a first, fundamental set of safety applications. In order to support vehicular communications in both in-coverage and out-of-coverage scenarios, LTE-V2X introduced two different resource allocation schemes known as Mode 3 and Mode 4. Mode 3 delegates the selection of collision-free radio resources to the evolved Node B (eNB), which coordinates the assignment of resources to all vehicles under cellular coverage. However, safety-critical applications cannot depend on the availability of the cellular infrastructure; hence, Mode 4 has been designed to allow vehicles to select resources via an autonomous and distributed approach that requires no eNB assistance.

In LTE-V2X Mode 4, vehicles communicate over a 10 or 20 MHz wide channel located in the 5.9 GHz Intelligent Transport System (ITS) band. At physical layer, Orthogonal Frequency Division Multiplexing (OFDM) is employed with a fixed 15 kHz subcarrier spacing, and transmission resources are arranged over the time-frequency resource grid exemplified in Fig. 1. The time unit is the subframe, whose duration is $t_s = 1$ ms, whereas the basic frequency unit is the Resource Block (RB), 180 kHz wide. A group of adjacent RBs within the same subframe is called a subchannel. In LTE-V2X, every packet is encapsulated within a Transport

Block (TB), whose transmission requires a different number of subchannels, depending on the TB size. Moreover, the transmission of each TB is complemented by the corresponding Sidelink Control Information (SCI), which contains decoding-critical information and is transmitted over two RBs, which are frequency-adjacent to the associated TB.

In Release 14, the Mode 4 resource allocation mechanism has been mainly tailored to serve periodic traffic. This is manifest in the Sensing-based Semi-Persistent Scheduling (SSPS) algorithm that the vehicles adopt for the distributed selection of transmission resources. The outcome of the SSPS mechanism is the selection – and reservation – of a collision-free Single-Subframe Resource (SSR), defined as the set of subchannels able to accommodate the transmission of the TB and of its associated SCI. Let us indicate the vehicle that needs to transmit a message and runs the SSPS algorithm as the ego-vehicle. The steps that it goes through are the following:

1. *List creation*: in the first phase, the ego-vehicle focuses on the Candidate Single-subframe Resources (CSRs) included within the selection window, W. As Fig.1 indicates, the selection window is the interval that goes from the time the packet is ready for transmission up to its latency deadline, dependent on the Packet Delay Budget (PDB). The ego-vehicle exploits the channel status information collected during the previous 1000 subframes, the so-called sensing window S, to learn which resources in W are already reserved by other vehicles. The ego-vehicle therefore builds a list, L_1, removing from the selection window the CSRs that satisfy the following two conditions: *(i)* the ego-vehicle has received an SCI indicating that the CSR will be used by another vehicle; *(ii)* the Reference Signal Received Power (RSRP) averaged over the RBs of the examined CSR is higher than a given threshold. Such threshold is a configurable parameter and its value is iteratively increased by 3 dB until list L_1 includes at least 20% of the initial CSRs. Last, the ego-vehicle builds a second list, L_2, including the top 20% of the CSRs in L_1 with the lowest average Received Signal Strength Indicator (RSSI). The RSSI value is averaged in a periodic fashion over the 10 previous occurrences of the examined CSR, equally spaced of 100 ms.
2. *Resource Selection and Reservation*: in the second phase, the ego-vehicle randomly selects an SSR from list L_2 and also randomly sets the reselection counter C_{resel} in $[C_{min}, C_{max}]$, indicating the consecutive number of times the resource will be reserved. For a packet periodicity $T \geq 100$ ms, $C_{min} = 5$ and $C_{max} = 15$ [27]. The time interval between consecutive reservations is termed Resource Reservation Interval (RRI), and it matches the packet generation period T, $RRI = T$. After each transmission, the reselection counter is decremented by one; when it expires, the SSPS algorithm is invoked again with probability $1 - P$, $P \in [0, 0.8]$ as indicated in [28].

Once the SSR has been selected, the ego-vehicle broadcasts the TB and the SCI, the latter including the RRI value. Neighboring vehicles are informed that the ego-vehicle intends to employ the same SSR for the next transmission after RRI ms, and avoid using that resource. If the ego-vehicle does not maintain the current reservation when the reselection counter expires, it notifies others by setting the RRI in the SCI equal to 0. Fig. 1 visually summarizes the relevant elements of the SSPS algorithm.

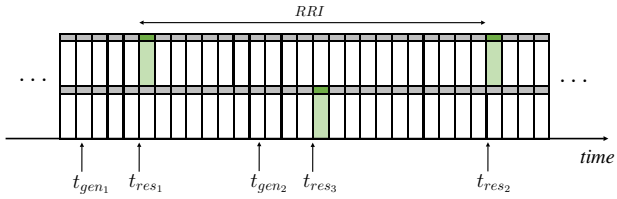

(a) Latency reselection

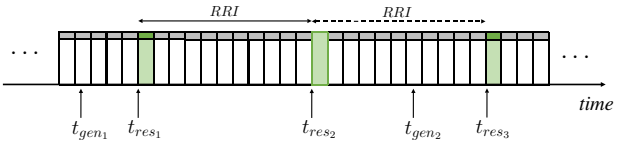

(b) Unused reservation

Fig. 2. Aperiodic traffic effects on LTE-V2X Mode 4 reservations

B. Impact of Aperiodic Traffic on Mode 4

When periodic traffic is examined, the RRI setting is a simple task, as the RRI has to match the packet generation period T. Depending on the value of the reselection probability P, Mode 4 is forced to select new resources only when C_{resel} expires; following the vocabulary in [10], this is an event termed *counter reselection* throughout this work. Note that the number of counter reselections a vehicle performs depends on the reselection probability P and on the average C_{resel} value.

However, when aperiodic traffic is considered, additional and unforeseen resource reselections can be triggered. Specifically, when resources are reserved with an RRI larger than the current packet inter-arrival time, then the so-called *latency reselections* [10] occur.

The situation is exemplified in Fig. 2(a): here, it is assumed that at t_{gen_1} an incoming packet triggers a counter reselection: the next two SSRs are reserved at t_{res_1} and t_{res_2}, $t_{res_2} = t_{res_1} + RRI$. Then, let next packet be generated at t_{gen_2}, $t_{gen_2} < t_{res_2}$, but $t_{res_2} - t_{gen_2} > PDB$; it follows that the reserved resource is not able to cope with the packet latency deadline. Therefore, a latency reselection is triggered at t_{gen_2}, and a new set of subchannels is selected and reserved at time t_{res_3} replacing the original reservation. Latency reselections should be avoided as much as possible, as they increase the probability of packet collisions.

Aperiodic traffic is also responsible for the phenomenon of *unused reservations* [10], which are observed when resources are reserved with an RRI lower than the current packet inter-arrival time. This circumstance is illustrated in Fig. 2(b), where the packet generated at t_{gen_1} triggers the reservation of resources at t_{res_1}, t_{res_2} and t_{res_3}, with $t_{res_2} = t_{res_1} + RRI$ and $t_{res_3} = t_{res_1} + 2RRI$. However, the second packet is generated at $t_{gen_2} > t_{res_2}$, hence leaving the reservation at t_{res_2} idle.

Unused reservations negatively affect Mode 4 performance in two different ways: first, a fraction of the overall system capacity is wasted, as the reserved resources are not utilized by either the ego-vehicle or the neighboring vehicles. Second, as shown in Fig. 2(b), the unused reservation at t_{res_2} does not allow the ego-vehicle to broadcast the corresponding SCI and announce the next reservation at t_{res_3}; the resources employed by the ego-vehicle at t_{res_3} are therefore sensed free from nearby users, increasing the risk of packet collisions.

To summarize, the RRI configuration is a key element for the proper operation of Mode 4 SSPS mechanism. Ideally, the RRI value should match the time pattern of the traffic profile, therefore varying over time. However, this task cannot be accomplished when aperiodic traffic is considered, and the inevitable mismatch can severely affect Mode 4 communication effectiveness. In this regard, the authors in [7] and [10] showed that the performance of LTE-V2X is degraded to a remarkable extent, when aperiodic messages are considered.

To the authors' knowledge, NR-V2X has not identified a solution to cope with aperiodic traffic. The question of how to accommodate such traffic type therefore remains open and it is addressed by the current work in the case of aperiodic CAM dissemination. To this aim, the next Section will elaborate on CAMs; the goal is to substantiate that CAMs are aperiodic, but their occurrence pattern can be forecast.

C. ETSI-Generated CAM Sequences

CAMs are facility-layer packets devised to regularly broadcast and exchange information among vehicles, and between vehicles and the roadside infrastructure. They represent the fundamental elements to build road safety and traffic efficiency applications [18]. When initially investigating LTE-V2X performance, CAM occurrences were modeled as periodic packets [29], a choice that perfectly suits the use of Mode 4. However, the standard algorithm for the generation of CAMs released by ETSI [18] indicates that the inter-arrival time between consecutive messages, T_{GenCAM}, is variable. Its duration strongly depends on the vehicle dynamics: if the vehicle modifies its trajectory, if its speed or acceleration/deceleration are sufficiently high, then T_{GenCAM} shortens and CAMs become more frequent. In greater detail, the ETSI algorithm defines the upper and lower bounds for T_{GenCAM}, namely:

$$T_{GenCAM_{Min}} \leq T_{GenCAM} \leq T_{GenCAM_{Max}} \quad (1)$$

where $T_{GenCAM_{Min}} = 100$ ms and $T_{GenCAM_{Max}} = 1000$ ms, the latter also representing the default value for the generation period. Within such limits, CAMs are triggered depending on the transmitting vehicle dynamics, which have to be sampled every $T_{CheckGenCAM}$ milliseconds, $T_{CheckGenCAM} \leq T_{GenCAM_{Min}}$. The typical setting is $T_{CheckGenCAM} = T_{GenCAM_{Min}} = 100$ ms. Specifically, a new CAM shall be immediately generated every time one of the following conditions is met [18]:

- the absolute difference between the current heading and the heading included in the previous CAM is greater than $4°$;
- the distance between the current position and the position included in the previous CAM is greater than 4 m;
- the absolute difference between the current speed and the speed included in the previous CAM is greater than 0.5 m/s;
- the time elapsed since last CAM generation is equal to or greater than $T_{GenCAM_{Max}}$.

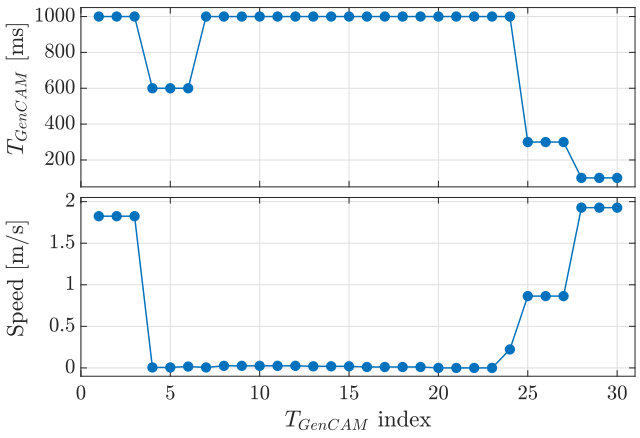

Fig. 3. Correlation between vehicular speed and T_{GenCAM}

Besides T_{GenCAM} specifications, [18] details the mandatory and optional fields in a CAM, allowing for variable size messages. The rules of the standard lead to CAM traffic which in most of the cases exhibits aperiodic inter-arrival times and variable CAM sizes. The last remark is well documented by the experimental survey in [30], which offers an analysis of CAMs collected during actual test-drives. The study reveals that CAM inter-arrival time often changes from one message to the next, that its distribution is very diverse, and heavily dependent on the drive scenario (urban, suburban, or highway). Similar conclusions hold for the size variability of CAMs. The correlation between CAM inter-arrival times and the vehicle behavior is exemplified in Fig. 3, where the temporal sequence of T_{GenCAM} values, i.e., a CAM trace, and the vehicle speed are reported as a function of the T_{GenCAM} sample index. These patterns refer to a vehicle moving along a straight trajectory, that initially decelerates until a complete stop, at T_{GenCAM} index $= 4$, and then starts to accelerate again from T_{GenCAM} index $= 23$, causing T_{GenCAM} to accordingly vary. Fig. 3 shows that when the vehicle decelerates (accelerates) in the first (last) portion of the CAM trace, CAMs are more frequently issued. On the other hand, T_{GenCAM} settles at 1000 ms when the vehicle stops, in the central portion of the trace. Here, variations in heading, position, or speed are not sufficiently large for generating a CAM before the timeout condition, $T_{GenCAM_{Max}} = 1000$ ms, occurs. Such a simple, yet exemplary instance is extracted from a wider measurement campaign we performed in different settings [31].

The strong correlation between CAM inter-arrival times and vehicle dynamics suggests that the adoption of ML can be beneficial to predict the temporal evolution of CAM sequences and in turn, lead to an effective reservation policy of radio

resources. Indeed, a carefully chosen set of input features, that the vehicle locally retrieves, can be used to feed an ML algorithm, producing the desired outcome, i.e., when next CAMs are likely to occur.

The following Section will therefore illustrate a novel approach to deliver aperiodic CAMs, removing the intrinsic inefficiencies that plague the original Mode 4.

III. The Predictive Reservation Framework

Subsection II-B highlighted the mismatch between aperiodic traffic and the periodic reservation strategy of Mode 4, causing the undesired phenomena of latency reselections and unused reservations. Moreover, Sec. II-C dwelled on the aperiodicity of actual CAM sequences, suggesting that their temporal evolution can be successfully predicted.

The key proposal of this paper is therefore the following: adopt ML to forecast what the next T_{GenCAM} value will be, and how many occurrences of it will appear. Next, exploit ML prediction to set: (i) the resource reservation interval RRI; (ii) the reselection counter C_{resel}, whose value is no longer randomly chosen, rather, it exactly matches the number of occurrences forecast by ML.

Additionally, the current study significantly intervenes in the list creation phase of the original SSPS algorithm. As better explained in the next subsection, it builds a more reliable list of available candidate resources than the one produced by the legacy SSPS.

A. Modified SSPS Implementation

In our proposed solution, resources are drawn from list L_1, as opposed to list L_2. As a matter of fact, in the presence of aperiodic traffic, L_2 is not as meaningful as when vehicles periodically generate packets. It is not a case that NR-V2X will no longer use L_2 [32]. Moreover, our proposal sets the selection window $W = 100$ ms, the minimum CAM inter-arrival time, to avoid broadcasting out-of-sequence messages. To better understand the last statement, recall that CAM inter-arrival times can take on any value in the $[100, 200, \ldots, 1000]$ ms set; hence, if the selection window W is wider than 100 ms, the $(j+1)$-th CAM might be transmitted before the j-th, an event that has to be prevented.

An additional and meaningful modification concerns the list creation phase of the original SSPS algorithm. Given the CAM selection window W is 100 ms wide and that the RRI is dynamically determined via ML, observe that not all ongoing reservations fall within W and are spotted by the ego-vehicle. It follows that the original SSPS list creation mechanism loses effectiveness, increasing the risk of packet collisions.

For this reason, we propose a new version of the SSPS process leading to the creation of list L_1, that we name *look-ahead* SSPS version. This SSPS reworking requires that the SCI also includes the current C_{resel} value, in addition to RRI. It is a minimal modification with respect to the choice of the legacy algorithm, necessitating very few bits. Yet, it remarkably extends the collision-avoidance capability of the original SSPS algorithm, as the numerical results will show.

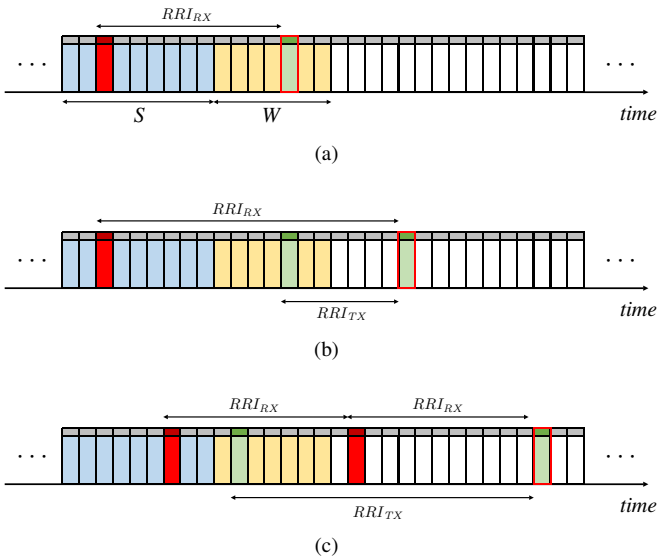

Fig. 4. SSPS detection of potential collisions for different RRI_{TX} and RRI_{RX} relations

As a matter of fact, if the ego-vehicle exploits the knowledge of the reselection counter of nearby vehicles, it can detect potential collisions for any possible combination of the resource reservation intervals used by itself and by its neighbors. To further clarify such enhanced capability of identifying collisions, Figs. 4(a)-(c) exemplify the SSPS operation in three different scenarios. In these figures, the candidate resources examined by the ego-vehicle are represented in green, the subchannels in use by the generic neighboring vehicle are indicated in red, the selection window in yellow. Furthermore, RRI_{TX} indicates the resource reservation interval adopted by the ego-vehicle, whereas RRI_{RX} represents the reservation interval of the generic nearby vehicle, heard by the ego-vehicle in the SCI it receives. In Fig. 4(a), the candidate resource examined by the ego-vehicle is immediately excluded, as it coincides with the reservation placed by the nearby vehicle inside the selection window. The collision is avoided in the case exemplified in Fig. 4(b) too, as the ego-vehicle also verifies if any of its future reservations outside of the selection window coincides with the very next resource reserved by the nearby vehicle. Fig. 4(c) portrays an instance where the reservation heard by the ego-vehicle is not included within its selection window and RRI_{RX} is lower than RRI_{TX}. In this case, the original SSPS algorithm cannot detect the future collision, as the ego-vehicle is exclusively aware of the first reservation from the neighboring vehicle, after RRI_{RX} ms, and therefore does not exclude the examined resource. Here, the future collision would be spotted only if the ego-vehicle additionally knew the remaining number of ongoing reservations, i.e., the current C_{resel} value of the nearby vehicle, in addition to the periodicity of ongoing transmissions. Our *look-ahead* version of SSPS proposes to exploit the C_{resel} knowledge and performs this further check. Therefore, it creates a smaller, yet more reliable L_1 list, detecting and avoiding all the potential collisions exemplified in Figs. 4(a)-(c).

B. Machine Learning to Predict CAM Sequences

When the proposed strategy enters the resource selection and reservation phase, the first step that the ego-vehicle accomplishes is to forecast through ML the very next T_{GenCAM} value, as well as the length of the next sequence of identical T_{GenCAM} inter-arrival times. To do so, ML explores a large set of CAM traces to identify correlation patterns between some user-defined input features and the CAM traces. Then, such knowledge is leveraged to anticipate future CAM inter-arrival times [33]. In this work, the set of input features taken into account are:

- trajectory, current speed and position of the ego-vehicle;
- current speed and position of the vehicle immediately preceding the ego-vehicle.

We choose to predict the next CAM inter-arrival time through the k-Nearest Neighbors (KNN) ML algorithm, an instance-based learning technique used for both regression and classification problems. KNN simply stores the training data without attempting to infer a general structure out of them. Moreover, KNN is inherently designed for multi-class problems and its classification consists in assigning the input features the most common label, i.e., next predicted T_{GenCAM} value, among the k nearest neighbors.

The second action of the ego-vehicle is to dynamically set the (RRI, C_{resel}) pair employed by the SSPS strategy in accordance to the ML forecast.

In greater detail, whenever SSPS triggers the resource selection and reservation phase, Algorithm 1 is invoked. The algorithm exploits KNN to predict the very next T_{GenCAM} value, T_{GenCAM_1}, and sets RRI equal to it, that is, $RRI = T_{GenCAM_1}$, while C_{resel} is initially set equal to 1. Then, as long as the next predicted inter-arrival time $T_{GenCAM_{i+1}}$ coincides with the previous T_{GenCAM_i}, the algorithm keeps incrementing the estimate of the reselection counter C_{resel}. Furthermore, when KNN outcome indicates that more than 3 consecutive CAM inter-arrival times will display the same value, the actual reselection counter value is randomly selected within the $[cntr_{min}, cntr_{max}]$ interval, where $cntr_{min} = 3$ and $cntr_{max}$ is the current C_{resel} estimate. This expedient avoids repeated packet collisions on resources reserved by different vehicles, a circumstance that might occur when vehicles generate CAMs with the same periodicity, e.g., in a congested intersection. The output of Algorithm 1 is finally used to set RRI and the reselection counter C_{resel} that indicates how many times the selected resource is reserved. Note that there is a maximum allowed value for C_{resel}, indicated by N. Moreover, observe that inequality $C_{resel} \geq 1$ reveals that at least one reservation has to be placed.

Algorithm 1: predictive reservation

Input : KNN input features
Output: RRI, C_{resel}

$i = 1$;
T_{GenCAM_i} = `Predict` (Input features, i);
RRI = T_{GenCAM_i};
$C_{resel} = 1$;
while $i \leq N$ **do**
  $i = i + 1$;
  T_{GenCAM_i} = `Predict` (Input features, i);
  if T_{GenCAM_i} = RRI **then**
    $C_{resel} = C_{resel} + 1$;
  else
    break;
  end
end
if $C_{resel} > 3$ **then**
  $C_{resel} = random[3, C_{resel}]$
end

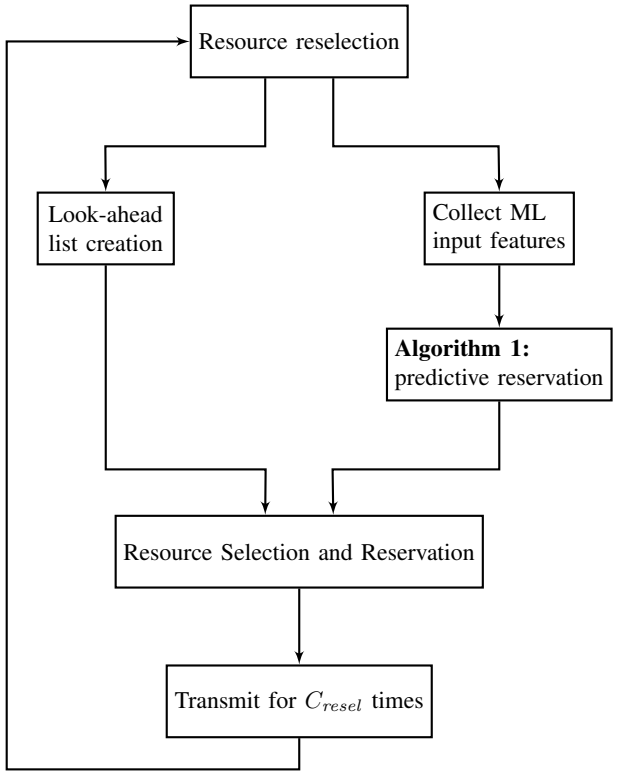

Fig. 5. Flowchart showing the proposed KNN-look ahead solution

The overall flowchart of the proposed solution, termed KNN-look ahead from now onward, is reported in Fig.5.

IV. Key Performance Indicators

When assessing the performance of a vehicular radio access solution, there are several Key Performance Indicators (KPIs) that are worth being considered.

One of the most widely adopted is the Packet Reception Ratio (PRR). Its definition relies on the notion of distance slice; the i-th distance slice is defined as the set of transmitter-receiver distances that fall within the $(a_i, b_i]$ range, $a_i = i \cdot 20$ m and $b_i = (i + 1) \cdot 20$ m. For the i-th slice, the PRR is defined as [29]:

$$PRR = \frac{\sum_{j=1}^{M} X_i^j}{\sum_{j=1}^{M} Y_i^j} \quad (2)$$

where X_i^j, indicates the number of vehicles within the i-th slice that successfully received the j-th packet, Y_i^j is the number of vehicles within the i-th slice when the j-th packet was transmitted and M denotes the number of packets generated during the simulation. The PRR is a reliability indicator, quantifying the probability that the message being broadcast by a vehicle can be heard at a given distance slice.

An additional standard-compliant reliability indicator is the Packet Inter-Reception (PIR). For a given transmitter-receiver pair, the PIR is defined as the time between two consecutive successful receptions of packets belonging to the same application flow, assuming the transmitter-receiver distance is within the $(0, D]$ range. Usually, its Cumulative Distribution Function (CDF) is provided, considering all transmitter-receiver pairs involved in the simulation.

Two additional KPIs are the Propagation Losses Ratio (PLR) and the Collision Losses Ratio (CLR). For the i-th slice, the PLR is defined as

$$PLR = \frac{PL_i}{PL_i + CL_i + SR_i} \tag{3}$$

and similarly, the CLR value is determined as

$$CLR = \frac{CL_i}{PL_i + CL_i + SR_i} \tag{4}$$

where:

- PL_i is the number of packets that were lost due to poor propagation conditions within the i-th slice, i.e., the packets that did not collide, but experienced a Signal-to-Noise Ratio (SNR) not sufficient for the correct decoding of either the TB or its associated SCI;
- CL_i is the number of packets lost within the i-th slice because of a collision, i.e., the packets that were caught in a collision and whose reception failed because the Signal-to-Interference-plus-Noise Ratio (SINR) did not allow a correct decoding of either the TB or the SCI.
- SR_i is the number of successfully received packets within the i-th slice.

In the following, subscript i will be omitted, unless strictly necessary.

We observe that the PLR measures the fraction of radio resources that could not be successfully employed because of errors introduced by lousy propagation conditions. As such, it is influenced by the choices performed at physical layer, by the channel model adopted in the geographical area that is being examined, and by the CAM size.

On the contrary, the CLR indicates to what extent harmful collisions could not be avoided, and it is therefore dictated by the radio resource assignment strategy.

A parameter also worth being monitored is the Channel Busy Ratio (CBR), which is defined as follows: given the n-th subframe, the CBR is the fraction of subchannels whose RSSI exceeds a given threshold over subframes $[n-100, n-1]$. The CBR is relevant to understand the load currently insisting on the radio channel. Additional metrics specific to LTE-V2X are [10]:

- the Latency Reselections Ratio (LRR), defined as the fraction of message transmissions that triggered a latency reselection over the total number of transmitted messages;
- the Unused Reservations Ratio (URR), defined as the fraction of unused reservations over the total number of resource reservations that were performed;
- the Counter Reselection Ratio (CRR), defined as the fraction of message transmissions that triggered a resource reselection due to the depletion of the reselection counter over the total number of transmitted messages.

V. Numerical Results

A. Physical and Medium Access Control Layer Configuration

As regards the Physical (PHY) and Medium Access Control (MAC) layers, this work relies on the custom ns-3 C-V2X module first introduced by the authors in [6] and finalized in [7]. The development of the simulator adheres to 3GPP Release 14 and Release 16 specifications and features all the elements that characterize Mode 4 communications. Vehicles have been configured to transmit their messages over the 10 MHz wide channel located in the 5.9 GHz ITS band, with 15 kHz subcarrier spacing. The 10 MHz channel is divided into 4 subchannels that consist of 12 RBs each, assuming adjacent transmission of the TB and of its associated SCI. The size of CAM messages, indicated by X, is fixed to either 190 or 470 bytes, which are the smallest and the largest statistically relevant sizes of CAMs [30]. Vehicles transmit their packets using QPSK modulation with 0.7 code rate, therefore mapping the 190 and 470 byte-long packets into 1 and 2 subchannels, respectively. The transmission power is set to 23 dBm and the receiver sensitivity to -90.4 dBm. As in [10], the RSRP threshold is -140 dBm. The PHY layer impairments introduced by the radio channel are captured using the 5G-compliant error model presented by the authors in [7]. In greater detail, shadowing is modeled via a lognormally distributed random variable and small-scale fading is evaluated using two different Clustered Delay Lines (CDL) corresponding to the Line-Of-Sight (LOS) and Non-Line-Of-Sight (NLOS) scenarios, as detailed in [29]. The Packet Error

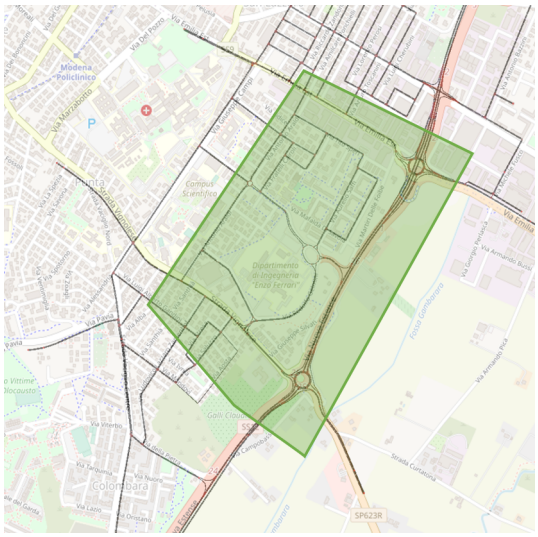

Fig. 6. The examined suburban road topology

Rate (PER) curve for the TB carrying the actual CAM and the associated SCI are reported in [7].

B. Outcomes

1) Suburban setting: The first set of results refer to some outskirts of the Italian city of Modena, that we classify as a suburban setting example. Here, microscopic vehicular mobility has been simulated through SUMO [34]. The examined road topology is reported in Fig. 6 and it has been imported in SUMO using Open Street Map [35]. The area is approximately 2.5 km wide and 3 km long. Vehicles have been randomly generated at the area edges and have been assigned random trajectories that traverse the entire topology. The average vehicular density is 42 vehicles/km and the vehicles speed varies in the $[50, 100]$ km/h interval, depending on traffic conditions and on the vehicle *speedFactor*, a SUMO parameter that defines the maximum velocity of each vehicle as a function of the lane speed limits.

We have additionally developed a set of custom tools based on the SUMO Traffic Control Interface (TraCI) [36], to extract the elements that characterize the behavior of every vehicle, namely, heading, position, and speed; the periodicity for their collection was coincident with $T_{GenCAM_{Min}} = 100$ ms. They have allowed us to generate CAM messages in accordance to the rules set by the ETSI algorithm recalled in Sec. II-C. For every car, we also recorded the position and speed of the preceding vehicle, to complete the set of input features used by ML. As requested by Algorithm 1, these features fed a real-time implementation of the KNN algorithm, to predict the longest sequence of T_{GenCAM} values with the same periodicity. The number k of KNN nearest neighbors was taken equal to 3.

The dataset of CAM traces was collected from a total of 6800 vehicles during 20 minutes of SUMO simulation. The least represented T_{GenCAM} values in the dataset were oversampled using the Synthetic Minority Oversampling TEchnique (SMOTE) [37]. All input features were further normalized using min-max normalization, i.e., their range of values was re-scaled between 0 and 1. The training set and the test set were generated employing a $70 - 30$ split ratio.

First, Figs. 7(a)-(c) delve into the ability of the KNN algorithm to predict the upcoming sequence of CAM messages, reporting the confusion matrix for three different values of the T_{GenCAM} index i, $i = 1, 5$ and 10. The confusion matrix is a two-dimensional matrix indexed with the true and predicted class labels, and it is commonly used to visualize the performance of an algorithm. Fig. 7(a) reports the confusion matrix of KNN for $i = 1$, that is, when KNN forecasts next T_{GenCAM} value. Figs. 7(b) and (c) show the confusion matrix when KNN predicts the fifth ($i = 5$) and the tenth ($i = 10$) T_{GenCAM} value, respectively. These figures reveal that KNN is able to accurately forecast T_{GenCAM_1} value, and that the degradation in predicting T_{GenCAM_5} and $T_{GenCAM_{10}}$ values is modest.

The goodness of the prediction outcomes is further highlighted by Fig. 8, that reports the accuracy (black curve, circle markers) and the macro-F1 score (red curve, square markers)

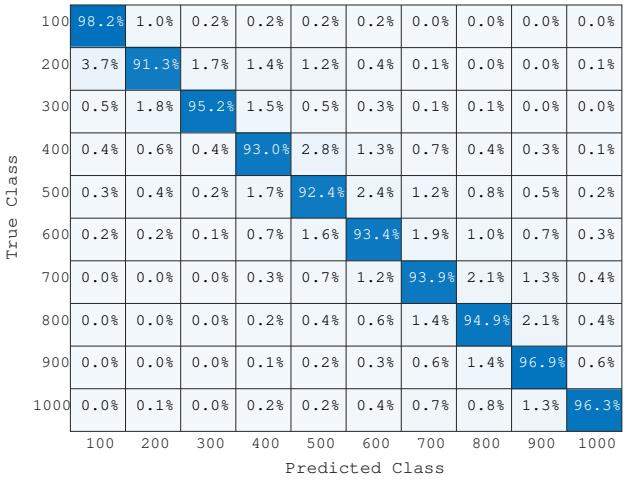

(a) T_{GenCAM_1}

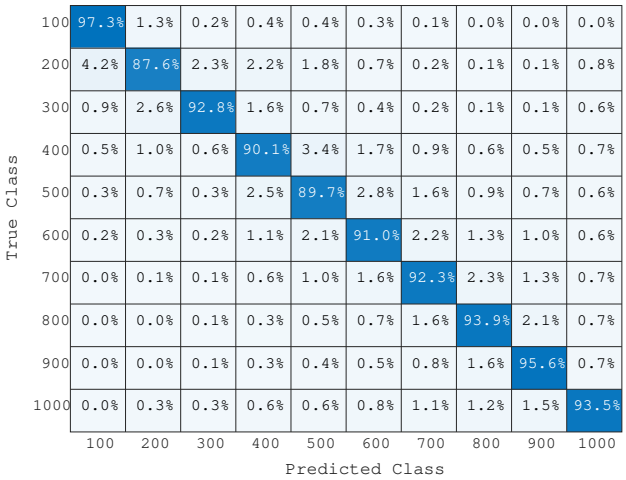

(b) T_{GenCAM_5}

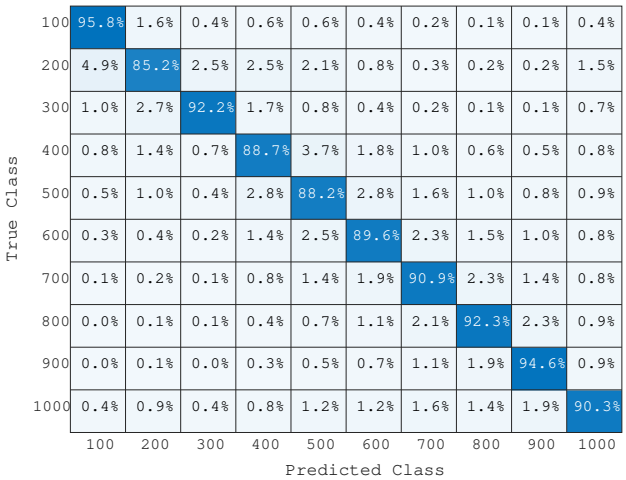

(c) $T_{GenCAM_{10}}$

Fig. 7. Confusion matrix for the prediction of the T_{GenCAM_i} values

of KNN as a function of i, $i = 1, 2 \ldots, N$, with $N = 10$. For a given T_{GenCAM} index i, the accuracy measures the fraction of correctly predicted T_{GenCAM} values over the total number of samples, and the macro-F1 score is the mean of class-wise F1-scores, where the F1-score is a common metric that combines

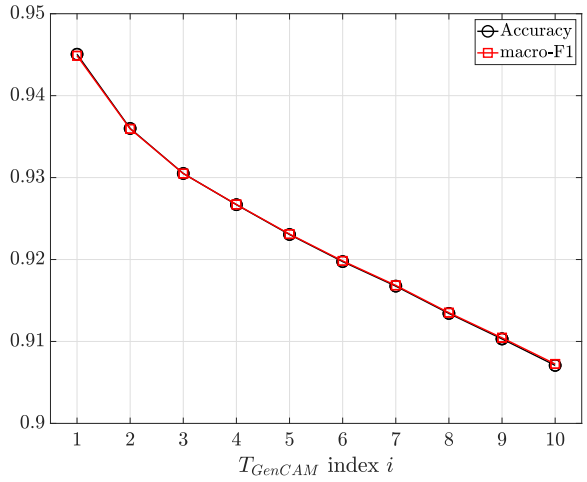

Fig. 8. Accuracy and macro-F1 score as a function of the T_{GenCAM} index

precision and recall [33]. As it could have been expected, KNN performance deteriorates for larger values of i, as the CAM inter-arrival time to be forecast is increasingly distant in time. However, both indicators settle on fairly high levels, greater than 0.9, even for $i = 10$.

In the next set of figures, the focus shifts on the performance of the proposed KNN-look ahead solution. First, Fig.9 shows the propagation losses ratio PLR as a function of the distance D between the transmitting and the receiving vehicle. Solid lines refer to $X = 470$, dashed lines to $X = 190$ bytes. Recall that the PLR measures the amount of packets that were lost because of scarce propagation conditions over the total; as a matter of fact, these curves do not depend on the resource assignment strategy, but are exclusively determined by the PHY layer choices and by the CAM size. So, when the radio propagation environment is more hostile (e.g., greater D values) and the CAM size is longer, the PLR increases. For these curves, as well as for the results shown next, a proper number of simulations has been executed to obtain sufficiently

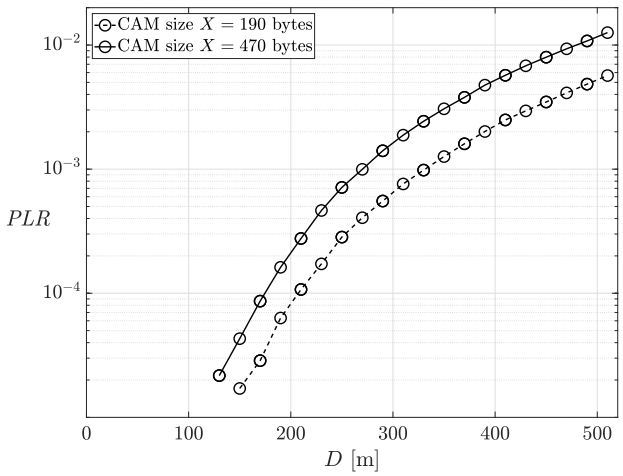

Fig. 9. PLR as a function of the Tx-Rx distance D

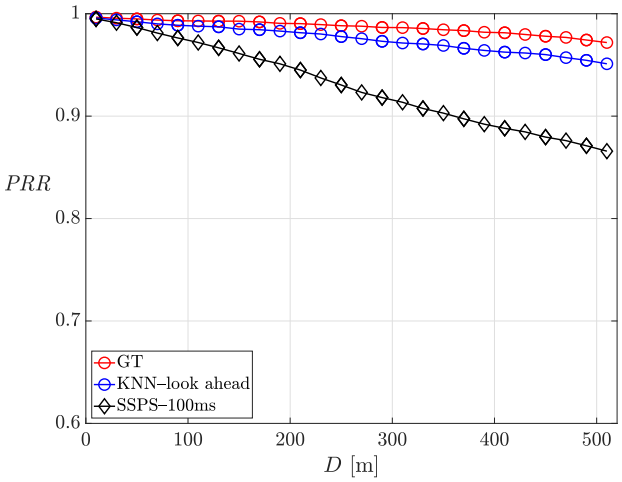

(a) CAM size $X = 190$ bytes

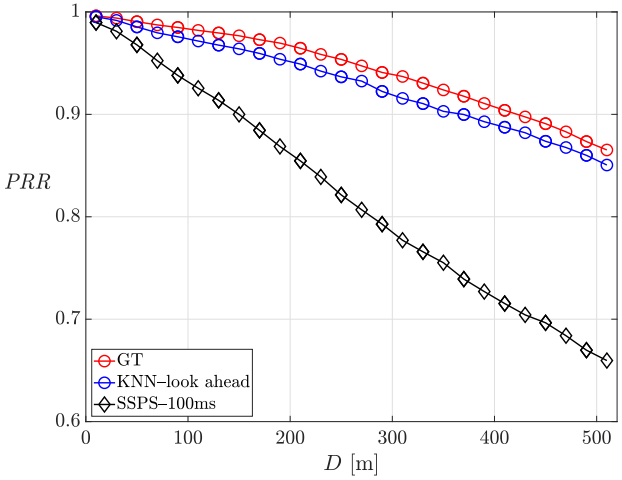

(b) CAM size $X = 470$ bytes

Fig. 10. PRR as a function of the Tx-Rx distance D, suburban scenario

tight 95% confidence intervals. To avoid border effects, the results have been collected only from the central area of the setting; this corresponds to the green-shaded area in Fig. 6.

In the following figures, the proposed approach is confronted against the original SSPS algorithm with $RRI = T_{GenCAM_{Min}} = 100$ ms; the latter is a convenient setting, as it guarantees that CAMs gain access to the channel without generating any latency reselections. Adhering to the standard, our SSPS implementation randomly chooses the actual C_{resel} value in $[5, 15]$. In accordance with [2], we set $P = 0$, that is, every time the counter expires, the vehicle has to select a new transmission resource with probability $1 - P = 1$.

To quantify how effective the KNN choice is within the ML domain, the Ground Truth (GT) benchmark is considered: this benchmark exploits the *a priori* knowledge of the CAM sequences to assign radio resources and place reservations that perfectly match the actual CAM sequences.

Figs. 10(a) and (b) report the PRR curves for the original SSPS mechanism with $RRI = 100$ ms (black curve, diamond markers), the curves obtained when the KNN-look ahead

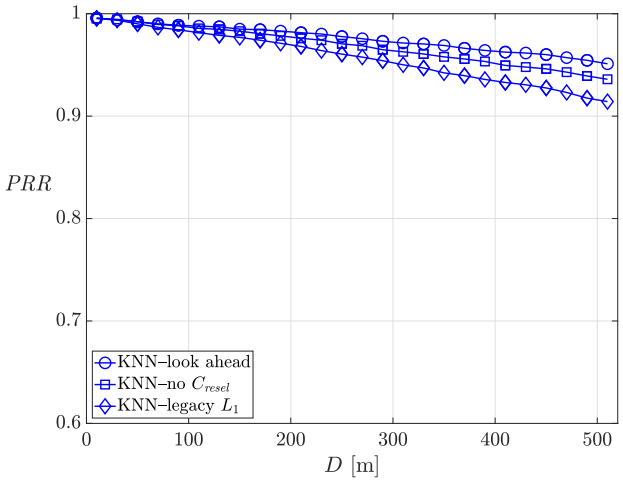

(a) CAM size $X = 190$ bytes

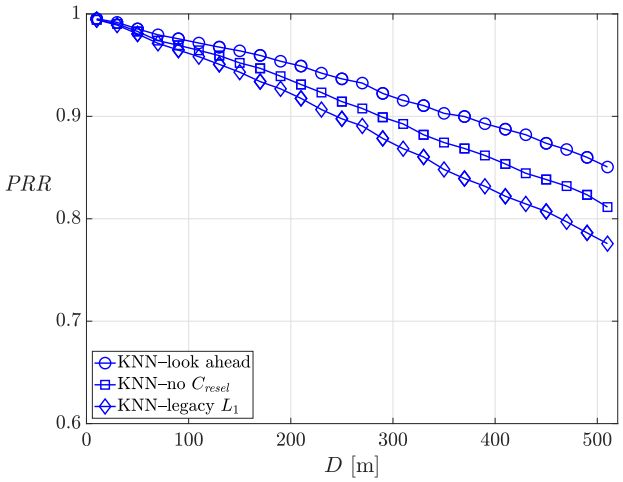

(b) CAM size $X = 470$ bytes

Fig. 11. PRR comparison for different L_1 lists, suburban scenario

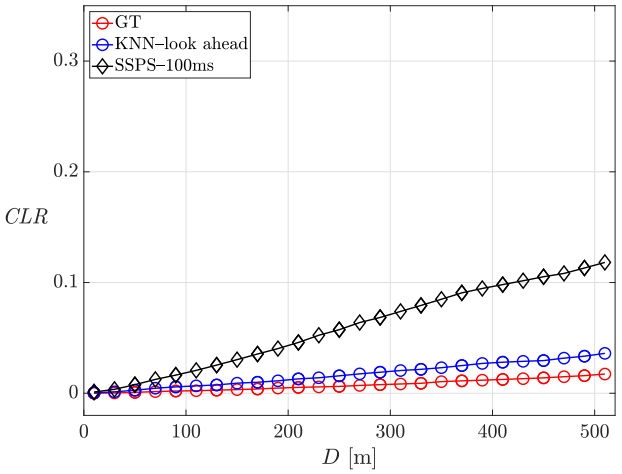

(a) CAM size $X = 190$ bytes

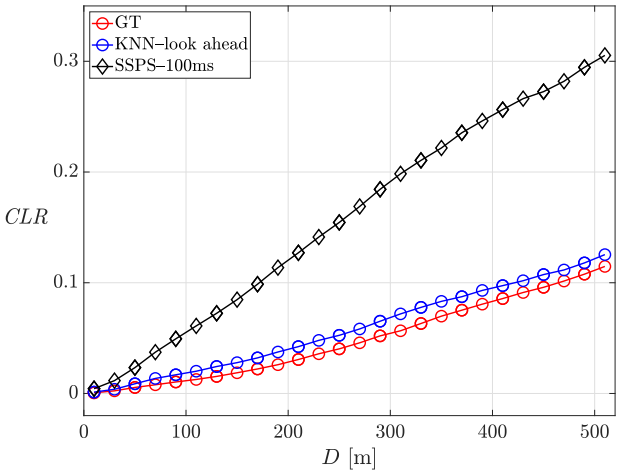

(b) CAM size $X = 470$ bytes

Fig. 12. CLR as a function of the Tx-Rx distance D, suburban scenario

proposal is adopted (blue curve, circle markers), as well as the PRR values corresponding to the ideal GT benchmark (red line, circle markers). When the CAM size is 190 bytes, Fig. 10(a) indicates that our proposal guarantees an attractive improvement, and Fig. 10(b) reveals that the gain becomes significant when a larger size ($X = 470$ bytes) is considered, that is, when the load on the radio channel increases. Both figures also reveal that the KNN-look ahead approach attains a performance that is very close to the GT benchmark, i.e., to the ideal performance.

Figs. 11(a) and (b) quantify the effects that different mechanisms for the creation of the L_1 list have on the KNN resource selection process, hence on PRR. In both figures, the lowest PRR curve refers to the solution that relies on the original L_1 list (solid curve, diamond markers); the intermediate curve refers to the alternative where the L_1 creation additionally concentrates on perspective collisions that might occur outside of the selection window W without exploiting the knowledge of C_{resel} (dashed line, square markers); the third, upper curve, to the proposed KNN look-ahead solution (dot-dashed, circle markers). These two figures indicate that the design choices summoned in our proposal consistently lead to the best performing approach.

Figs. 12(a) and (b) offer a further insight, displaying the CLR curves for the same choice of parameters as in Figs. 10(a) and (b). Coherently, the proposed KNN-look ahead strategy displays the lowest CLR values. These figures additionally reveal that the CLR values of the GT benchmark are not zero for all D values. The existence of a CLR "floor" is justified observing that, even if every vehicle were able to perfectly forecast its CAM transmission requirements over time and to select resources accordingly, its selection could nevertheless coincide with the choice performed by other vehicles. This phenomenon is intrinsic to the distributed nature of the channel access mechanism and cannot be further reduced, unless a total redesign of the radio access technique is undertaken.

The effectiveness of the KNN-look ahead approach is further evidenced by the values provided in Table I, where the Latency Reselections Ratio LRR and the Unused Reservations Ratio URR of the proposed solution are compared against the

TABLE I
SUBURBAN SCENARIO: URR, LRR AND CRR VALUES

	URR	LRR	CRR
SSPS, RRI=100 ms	0.61	0.0	0.18
KNN-look ahead	0.12	0.10	0.22
Ground Truth	0.0	0.0	0.34

values of these ratios for the original SSPS mechanism with $RRI = 100$ ms and for the GT benchmark.

The Table shows that SSPS with $RRI = 100$ guarantees no latency reselections, as it respects the most stringent delay requirement, but the URR climbs to 0.61. At the other end of the scale, the GT benchmark perfectly eliminates unused reservations and reselections. The proposed solution lies in between, being able to significantly reduce the unused reservations ratio from 0.61 to 0.12. However, this improvement is achieved at the expense of a non-zero fraction of latency reselections. It is worth noting that, as long as they are not prevalent, latency reselections do not have the same negative impact on communication reliability as unused reservations. For the sake of completeness, the Counter Reselection Ratio CRR is also reported in the last column of the table: as expected, its value increases for the proposed solution and even more for the GT benchmark, as reselections become more frequent to track T_{GenCAM} variability.

Next, Fig. 13 reports the Probability Mass Function (PMF) of the T_{GenCAM} values observed in the suburban scenario. It is interesting to note that the PMF mainly concentrates around two values, 200 ms and 300 ms. As they are not integer multiples, the SSPS algorithm with RRI set equal to 100 ms is not very effective in detecting potential collisions. This explains why we observed fairly low PRR values for it.

Given the *a posteriori* knowledge that the PMF reported in Fig. 13 provides, Fig. 14 shows the PRR attained by the legacy SSPS strategy when its reservation periodicity RRI is set so as to match the first or the second most frequently observed T_{GenCAM} value; that is, $RRI = 300$ ms (dashed

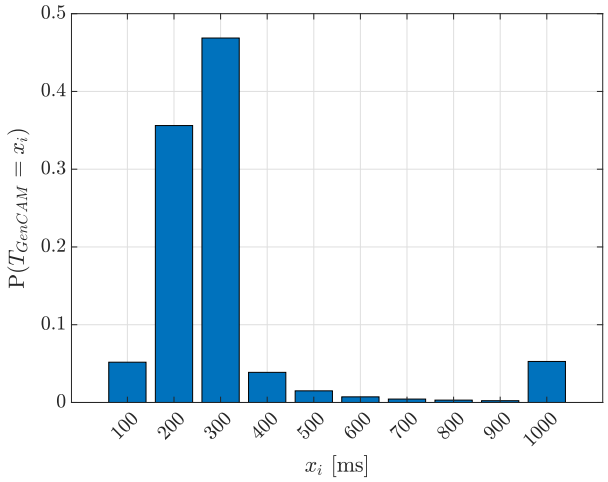

Fig. 13. T_{GenCAM} PMF, suburban scenario

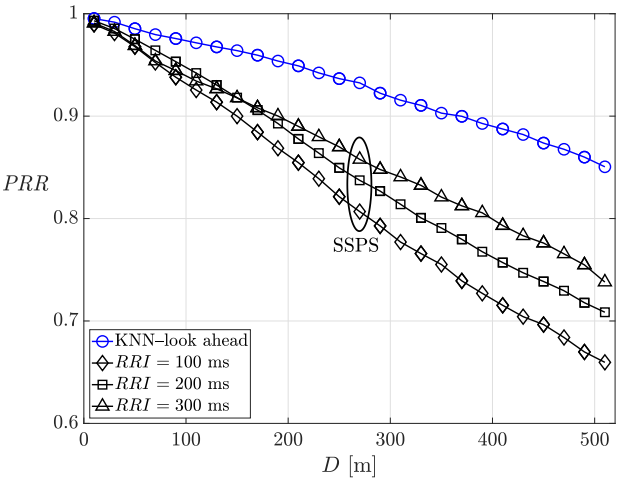

Fig. 14. PRR comparison against SSPS with different RRI settings, suburban scenario

black line) and $RRI = 200$ ms (dot-dashed black line). Such PRR values are further confronted against the baseline performance provided by SSPS with $RRI = 100$ ms (solid black line), and against the performance that the proposed KNN-based look ahead solution attains (blue line). Tuning the reservation periodicity improves the PRR of the legacy SSPS algorithm: unfortunately, the most proper RRI selection would be possible only if the T_{GenCAM} PMF were *a priori* known. Instead, KNN – or any alternative ML choice – does not necessitate such knowledge and yet, provides far higher PRR levels.

To further complete the assessment picture, Table II reports the CBR levels observed in the suburban scenario. The CBR of the generic vehicle has been computed every 0.2 seconds, the values have been time averaged over the central portion of the simulation time and finally averaged over all vehicles. The RSSI threshold to discriminate between a busy and an idle channel is set to a value 0.5 dB greater than the receiver sensitivity level, therefore to -89.9 dBm. The CBR values reported in Table II reveal the magnitude of the channel load increase due to a larger packet size. Moreover, the CBR is not only useful for assessing the amount of traffic insisting on the communication channel. Given a specific setting, the CBR also reflects the effectiveness of the adopted access strategy: a more accurate scheduling mechanism maximizes the use of the available transmission resources, resulting in larger CBR values. This is the case encountered here, where the KNN-look ahead approach achieves higher CBR values than SSPS with 100 ms.

TABLE II
SUBURBAN SCENARIO: CBR VALUES

	$X = 190$	$X = 470$
SSPS, RRI=100 ms	0.24	0.4
KNN-look ahead	0.26	0.46
Ground Truth	0.27	0.47

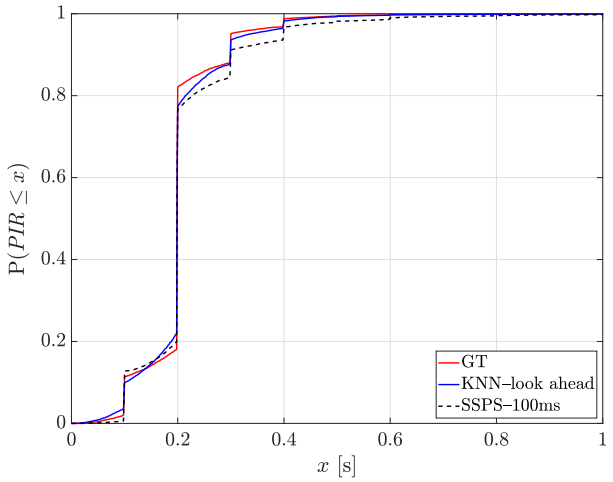

(a) CAM size $X = 190$ bytes

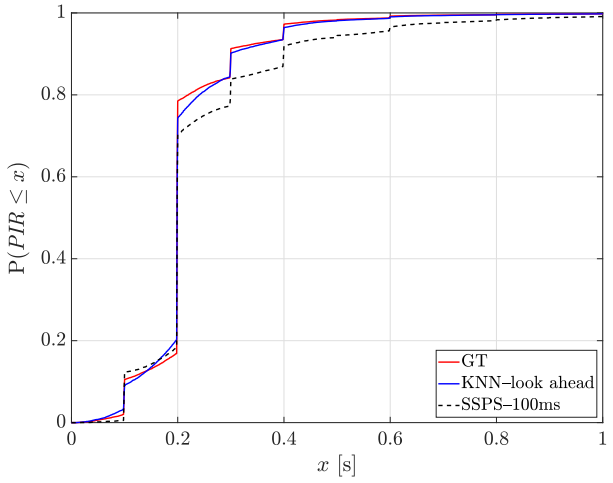

(b) CAM size $X = 470$ bytes

Fig. 15. *PIR* CDF, suburban scenario

Figs. 15(a) and (b) show the *PIR* Cumulative Distribution Function (CDF) when $D = 520$ m, for the GT benchmark (red curve), for the proposed KNN-look ahead solution (blue curve) and for the legacy SSPS (black curve). When $X = 470$ bytes, Fig. 15(b) indicates that the probability of observing *PIR* values lower than 200 ms and 300 ms, the two most frequent T_{GenCAM} values, is 0.74 and 0.90 for the KNN-look ahead solution. This is an improvement with respect to the values of the original SSPS implementation, equal to 0.70 and 0.84, respectively. Moreover, the discrete nature of the T_{GenCAM} values in the $[100, 1000]$ ms range reflects in the step behavior of the *PIR* CDF.

2) Highway setting: We also considered a second setting, termed *highway*, represented by a 5 km-long highway trunk, where six 4-meter wide lanes are deployed. Adhering to the specifications in [29], the vehicles' speed is 70 km/h and the vehicular density is 120 vehicles/km. For these numerical choices, Fig. 16 compares the PRR of the proposed KNN-look ahead solution to the PRR of the SSPS algorithm with $RRI = 100$ ms and to the GT upper bound, for the most demanding CAM size $X = 470$ bytes. The figure

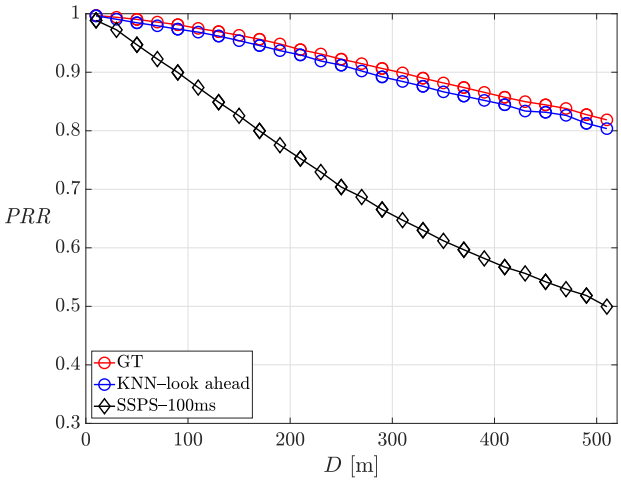

Fig. 16. *PRR* as a function of the Tx-Rx distance D, highway scenario, CAM size $X = 470$ bytes

shows that the KNN-look ahead approach (blue line, circle markers) leads to a remarkable improvement in the PRR performance with respect to the original SSPS mechanism (black line, diamond markers), achieving PRR levels very close to the GT benchmark (red line, circle markers). It is however known that SUMO reveals some limits in the highway set-up: the constant speed and the nearly straight vehicular trajectories lead to an almost constant CAM inter-arrival time, $T_{GenCAM} = 300$ ms. The same behavior was observed when the vehicular speed varies within the $[70, 140]$ km/h range: here too, T_{GenCAM} is nearly constant and equal to 200 ms. We have overcome this simulation hurdle employing one of the empirical models for the generation of CAM messages that were proposed in [38]. These models are derived from real-world traces of CAM traffic collected on a highway trunk [30], for different implementations of the ETSI algorithm by two Original Equipment Manufacturers (OEMs), Volkswagen and Renault. They consist of m-th order Markov sources that model: (i) CAM size and T_{GenCAM} variability; (ii) CAM size

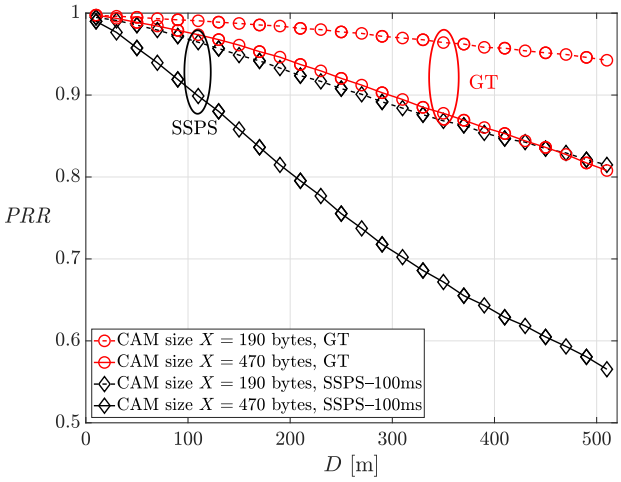

Fig. 17. *PRR* as a function of D, highway scenario, CAM trace Markov model

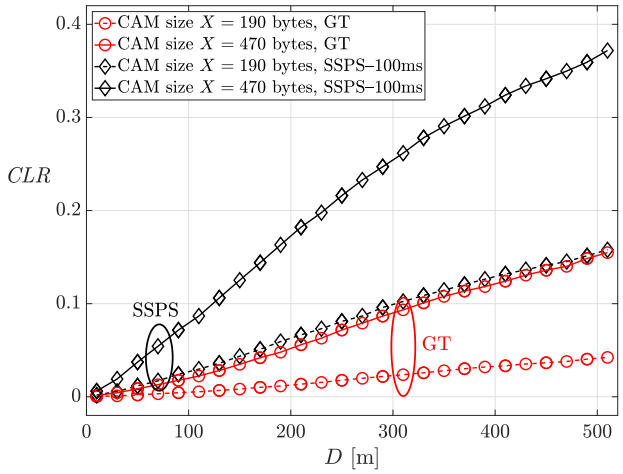

Fig. 18. CLR as a function of D, highway scenario, CAM trace Markov model

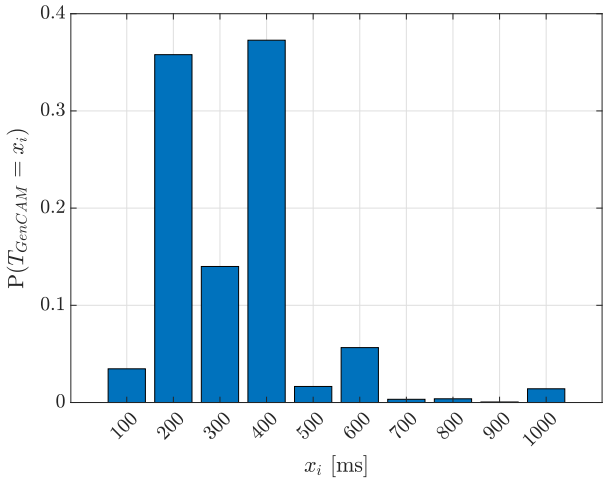

Fig. 19. T_{GenCAM} PMF, highway scenario

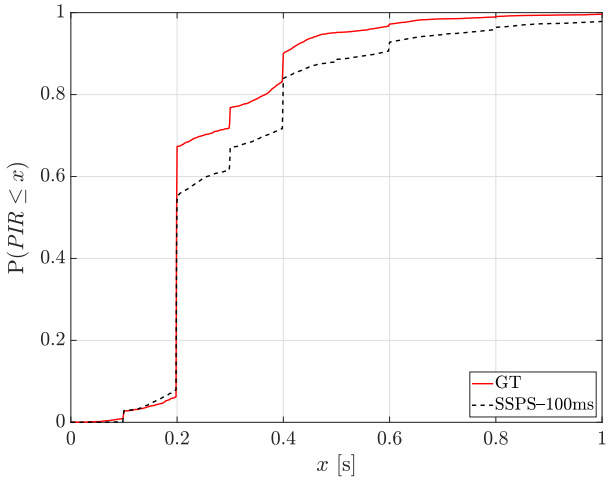

Fig. 20. PIR CDF, CAM size $X = 470$ bytes, highway scenario

variability only; (iii) T_{GenCAM} variability only. We adopted the model that seizes CAM temporal variability, drawn from the Volkswagen CAM traces, setting $m = 5$. For this model, the average T_{GenCAM} value is 330 ms, close to the constant T_{GenCAM} value characterizing the SUMO implementation at 70 km/h constant speed. With the help of this analytical tool, we associated to every vehicle a specific CAM trace. Unfortunately, such empirical models have no notion of vehicle dynamics, so they do not provide the input features the KNN algorithm requires. Nonetheless, the reproduction of highway CAM traces allows to determine the GT performance, and therefore to assess the maximum improvement that ML achieves. In this respect, Fig. 17 concentrates on the PRR performance considering two different packet sizes, $X = 190$ bytes (dashed lines) and $X = 470$ bytes (solid lines). Adopting the same choice of colors and markers of Figs. 10(a)-(b), the black curves correspond to the original SSPS implementation with $RRI = 100$ ms, whereas the red curves refer to the GT benchmark, identifying the PRR upper bound. The significant improvement achieved by the GT solution with respect to the original SSPS mechanism is evident and becomes remarkable when $X = 470$ is considered. The original SSPS performance drops below 0.6 when $D \geq 450$ m, whereas the GT sets at $PRR = 0.85$. Fig. 18 is the counterpart of Fig. 17 on the (CLR, D) plane. This figure further highlights the enhanced collision-avoidance capability of the ML-based strategy with respect to the standard-compliant solution, that increases for increasing packet sizes. Its superiority is substantiated by the CBR values reported in Table III. The first column of the Table refers to $X = 190$ bytes: the CBR increases from 0.34 to 0.39 when moving from SSPS with $RRI = 100$ ms to the GT benchmark. Likewise, the CBR rises from 0.49 to 0.61 in the second column that refers to $X = 470$ bytes, once more highlighting the significant impact of T_{GenCAM} predictions on the selection of collision-free resources.

TABLE III
HIGHWAY SCENARIO: CBR VALUES

	$X = 190$	$X = 470$
SSPS, RRI=100 ms	0.34	0.49
Ground Truth	0.39	0.61

The PMF of the T_{GenCAM} samples generated in the highway scenario is shown in Fig. 19. As in the suburban setting, the PMF mainly condenses around two values, 200 ms and 400 ms. Finally, Fig. 20 reports the PIR CDF when $D = 520$ m and $X = 470$ bytes. Here too, the GT benchmark provides an upper bound to the PIR achievable performance, highlighting the maximum amount of improvement with respect to the original SSPS reservation strategy.

It is worth observing that the implementation of the proposed approach on an actual vehicle is feasible, as the input features that KNN employs can be easily retrieved. The ego-vehicle position can be obtained via the Global Navigation Satellite System (GNSS), its speed can be measured by in-vehicle sensors, the use of on-board lidars and radars can offer accurate estimates of the position and speed of the

preceding vehicle. The vehicle trajectory prediction is a widely investigated topic in the industrial and the academic world, and algorithms like the one reported in [39] can estimate the ego-vehicle trajectory in an accurate manner.

As regards the introduction of ML, we showed that a simple technique such as KNN leads to a remarkable performance improvement with respect to the original LTE-V2X Mode 4. The selection of a more sophisticated ML algorithm, although possible, would only lead to incremental improvements and to unnecessary complexity.

VI. Conclusions

In this paper, an ML-based solution has been proposed to distribute aperiodic CAMs to vehicles. The approach relies on a limited set of features, that each vehicle employs to forecast its next CAM generation times. The ML outcome is combined with a careful selection and reservation of the radio resources available for transmission. The simulation results indicate that the proposed KNN-look ahead solution achieves an excellent accuracy and that the new strategy outperforms the legacy 3GPP V2V approach for all metrics.

References

[1] A. Bazzi, G. Cecchini, A. Zanella, and B. M. Masini, "Study of the impact of PHY and MAC Parameters in 3GPP C-V2V Mode 4," *IEEE Access*, vol. 6, pp. 71685-71698, 2018.

[2] M. Gonzalez-Martín, M. Sepulcre, R. Molina-Masegosa and J. Gozalvez, "Analytical Models of the Performance of C-V2X Mode 4 Vehicular Communications," *IEEE Trans. on Veh. Technol.*, vol. 68, no. 2, pp. 1155-1166, Feb. 2019.

[3] A. Bazzi, C. Campolo, A. Molinaro, A. O. Berthet, B. M. Masini and A. Zanella, "On Wireless Blind Spots in the C-V2X Sidelink," *IEEE Trans. on Veh. Technol.*, vol. 69, no. 8, pp. 9239-9243, Aug. 2020.

[4] F. Abbas, P. Fan and Z. Khan, "A Novel Low-Latency V2V Resource Allocation Scheme Based on Cellular V2X Communications," *IEEE Trans. on Intell. Transp. Syst.*, vol. 20, no. 6, pp. 2185-2197, June 2019.

[5] V. V. Chetlur and H. S. Dhillon, "Coverage and Rate Analysis of Downlink Cellular Vehicle-to-Everything (C-V2X) Communication," *IEEE Trans. on Wireless Commun.*, vol. 19, no. 3, pp. 1738-1753, March 2020.

[6] L. Gibellini and M. L. Merani, "Out-of-Coverage multi-hop road safety message distribution via LTE-A cellular V2V (C-V2V)," in *Proc. IEEE 88th Vehicular Technology Conference (VTC-Fall)*, Chicago, IL, USA, Aug. 2018, pp. 1-6.

[7] L. Lusvarghi and M. L. Merani, "On the Coexistence of Aperiodic and Periodic Traffic in Cellular Vehicle-to-Everything," *IEEE Access*, vol. 8, pp. 207076-207088, 2020.

[8] S. Bartoletti, B. M. Masini, V. Martinez, I. Sarris and A. Bazzi, "Impact of the Generation Interval on the Performance of Sidelink C-V2X Autonomous Mode," *IEEE Access*, vol. 4, pp. 35121 - 35135, 2021.

[9] L. Lusvarghi and M. L. Merani, "MoReV2X - A New Radio Vehicular Communication Module for ns-3," Sept. 2021, TechRxiv.

[10] R. Molina-Masegosa, J. Gozalvez and M. Sepulcre, "Comparison of IEEE 802.11p and LTE-V2X: An Evaluation With Periodic and Aperiodic Messages of Constant and Variable Size," *IEEE Access*, vol. 8, pp. 121526-121548, 2020.

[11] F. Hussain, R. Hussain, A. Anpalagan and A. Benslimane, "A New Block-Based Reinforcement Learning Approach for Distributed Resource Allocation in Clustered IoT Networks," *IEEE Trans. on Veh. Technol.*, vol. 69, no. 3, pp. 2891-2904, March 2020.

[12] H. Xiang, M. Peng, Y. Sun and S. Yan, "Mode Selection and Resource Allocation in Sliced Fog Radio Access Networks: A Reinforcement Learning Approach," *IEEE Trans. on Veh. Technol.*, vol. 69, no. 4, pp. 4271-4284, April 2020.

[13] H. Ye, Y. Li and B.-H. F. Juang, "Deep Reinforcement Learning based Resource Allocation for V2V Communications," *IEEE Trans. on Veh. Technol.*, vol. 68, no. 4, pp. 3163-3173, April 2019.

[14] H. Ye, L. Liang, G. Ye Li, J. Kim, L. Lu and M. Wu, "Machine Learning for Vehicular Networks: Recent Advances and Application Examples," *IEEE Veh. Technol. Mag.*, vol. 13, no. 2, pp. 94-101, June 2018.

[15] F.A. Ghaleb *et al*., "Deep Kalman Neuro Fuzzy-Based Adaptive Broadcasting Scheme for Vehicular Ad Hoc Network: a Context-Aware Approach," *IEEE Access*, vol. 8, pp. 217744-217761, Dec. 2020.

[16] J. Aznar-Poveda, E. Egea-López and A. J. García-Sanchez, "Cooperative Awareness Message Dissemination in EN 302 637-2: an Adaptation for Winding Roads," *2020 IEEE 91st Veh. Technol. Conf. (VTC2020-Spring)*, 2020, pp. 1-5.

[17] O. Amador, I. Soto, M. Uruena and M. Calderon, "GoT: Decreasing DCC Queueing for CAM Messages," *IEEE Commun. Lett.*, vol. 24, no. 12, pp. 2974-2978, December 2020.

[18] European Telecommunications Standards Institute (ETSI), "Intelligent Transport Systems (ITS); Vehicular Communications; Basic Set of Applications; Specification of Cooperative Awareness Basic Service," EN 302 637-2 V1.4.1, April 2019.

[19] M. Sepulcre, J. Gozalvez, G. Thandavarayan, B. Coll-Perales, J. Schindler and M. Rondinone, "On the Potential of V2X Message Compression for Vehicular Networks," *IEEE Access*, vol. 8, pp. 214254-214268, December 2020.

[20] A. Bazzi, A. Zanella and B. M. Masini, "Optimizing the Resource Allocation of Periodic Messages with Different Sizes in LTE-V2V," *IEEE Access*, vol. 1, pp. 43820-43830, March 2019.

[21] A. Bazzi, C. Campolo, B. M. Masini, A. Molinaro and A. Zanella, "Enhancing Cooperative Driving in IEEE 802.11 Vehicular Networks Through Full-Duplex Radio," *IEEE Trans. on Wireless Commun.*, vol. 17, No. 4, pp. 2402-2416, April 2018.

[22] N. Lyamin, A. Vinel, M. Jonsson and B. Bellalta, "Cooperative Awareness in VANETs: on ETSI EN 302 637-2 Performance," *IEEE Trans. on Veh. Technol.*, vol. 67, no. 1, pp. 17-28, Jan. 2018.

[23] G. Giambene, M. S. Rahman and A. Vinel, "Analysis of V2V Sidelink Communications for Platoon Applications," *ICC 2020 - 2020 IEEE Int. Conf. on Commun. (ICC)*, 2020, pp. 1-6.

[24] S. Roger *et al.*, "Low-Latency Layer-2-Based Multicast Scheme For Localized V2X Communications," *IEEE Trans. on Int. Transp. Syst.*, vol. 20, no. 8, pp. 2962-2975, Aug. 2019.

[25] B. Coll-Perales, J. Gozalvez, M. Gruteser, "Sub-6GHz Assisted MAC for Millimeter Wave Vehicular Communications," *IEEE Commun. Mag.*, vol. 57, no. 3, pp. 125-131.

[26] Z. Li, L. Xiang, X. Ge, G. Mao and H. -C. Chao,"Latency and Reliability of mmWave Multi-Hop V2V Communications Under Relay Selections," *IEEE Trans. on Veh. Technol.*, vol. 69, no. 9, pp. 9807-9821, Sept. 2020.

[27] 3GPP, "NR; Medium Access Control (MAC) protocol specification," TS 38.321, Rel-16 V16.4.0, Mar. 2021.

[28] 3GPP, "NR; Radio Resource Control (RRC) protocol specification," TS 38.331, Rel-16 V16.3.1, Jan. 2021.

[29] 3GPP, "Study on evaluation methodology of new Vehicle-to-Everything (V2X) use cases for LTE and NR," TR 37.885, Rel-15 V15.3.0, Jun. 2019.

[30] CAR 2 CAR Communication Consortium, "Survey on ITS-G5 CAM statistics," TR2052, V1.0.1, Dec. 2018.

[31] L. Zucchini, "Vehicular Safety Communications," B.S. thesis, Department of Engineering "Enzo Ferrari", University of Modena and Reggio Emilia, July 2020.

[32] M. H. C. Garcia *et al.*, "A Tutorial on 5G NR V2X Communications," *IEEE Commun. Surveys & Tutorials*, vol. 23, no. 3, pp. 1972-2026, 3rd quarter 2021.

[33] P. Harrington, *Machine Learning in Action*, Manning Publications, April 2012.

[34] P. A. Lopez, E. Wiessner, M. Behrisch, L. Bieker-Walz, J. Erdmann, Y.-P. Flotterod, R. Hilbrich, L. Lucken, J. Rummel, and P. Wagner, "Microscopic traffic simulation using SUMO," in *Proc. 21st Int. Conf. Intell. Transp. Syst. (ITSC)*, Maui, HI, USA, Nov. 2018, pp. 2575-2582.

[35] OpenStreetMap contributors (2020). https://www.openstreetmap.org/

[36] A. Wegener, M. Piorkowski, M. Raya, H. Hellbruck, S. Fischer and J. Hubaux, "TraCI: An Interface for Coupling Road Traffic and Network Simulators," in *11th Commun. and Netw. Siml. Symp. (CNS)*, 2008.

[37] N. V. Chawla, K. W. Bowyer, L. O. Hall and W. P. Kegelmeyer, "SMOTE: synthetic minority over-sampling technique," *Journal of Artif. Intell. Res.*, Jan. 2002, pp. 321-357.

[38] R. Molina-Masegosa, M. Sepulcre, J. Gozalvez, F. Berens, and V. Martinez, "Empirical models for the realistic generation of cooperative awareness messages in vehicular networks," *IEEE Trans. on Veh. Technol.*, vol. 69, no. 5, pp. 5713-5717, May 2020.

[39] A. Houenou, P. Bonnifait, V. Cherfaoui and W. Yao, "Vehicle trajectory prediction based on motion model and maneuver recognition," in *2013 IEEE/RSJ Int. Conf. on Intell. Robots and Systems*, Tokyo, 2013, pp. 4363-4369.

AE:

After careful consideration of the reviewers' comments, the decision has been made not to publish this paper in the IEEE Transactions on Vehicular Technology. Based on the reviewers' comments and my own opinion, the publication of the paper in its present form is not recommended. Reviewer 1 has concerns about the novelty of the work as per the existing state-of-the-art. Reviewer 2 has concerns about the motivations of the work. Furthermore, reviewer 3 also has found issues in describing the use of ML in the scheme. In addition to the reviewer's comments, I strongly recommend to compare the proposed scheme with recent related works as mentioned in the paper.

Authors response to the Associate editor

Dear editor,

thank you for allowing a resubmission of our manuscript, with an opportunity to reply to the reviewers' comments. We revised the manuscript, striving to address the remarks of all reviewers in a careful manner.

In summary:

- *the novelty of our approach and a critical comparison between its contributions and the existing works was provided;*
- *the Introduction was significantly modified, to better motivate our work. Several new paragraphs were introduced, to provide a critical review of the state of the art;*
- *the body of references was revised and increased;*
- *the rationale behind the adoption of Machine Learning (ML) was provided.*

Moreover, the manuscript was revised by an English-mother tongue, to remove grammatical errors and awkward sentence structures.

We also addressed the reviewer's concerns on a point-to-point basis, as reported below.

We are therefore re-submitting the revised manuscript as a new submission and do look forward to receiving your feedback soon.

Best regards,

Luca Lusvarghi *Maria Luisa Merani*

Authors response to the reviewers

Reviewer: 1

Reviewer #1 concern #1: The authors focus on ML-based CAM dissemination in cellular vehicular networks. The main concern is the rationale for using ML. Why do the authors think

the existing mechanisms (there are a lot of existing works addressing CAM dissemination and they achieve good results.
There is no related work in this paper which is why it is hard to convince oneself about the outperformance of this scheme. Therefore, through related work analysis is needed and the need for 'yet another' CAM dissemination scheme should be justified.

Author response: *We thank the reviewer for his/her comment. In the revised manuscript, we added an extensive state-of-the-art section, to evidence that there are no proposals in literature that address the issues of disseminating real CAM traffic. As of today, the topic of Cooperative Awareness Message (CAM) dissemination has only been investigated considering unrealistic, periodic CAMs with fixed size. The detrimental impact of aperiodic traffic on LTE-V2X Mode 4 performance has been recently highlighted by ourselves in [ACCESS-LUSVARGHI] and by Molina-Masegosa et al. in [MOLINA]. To the authors' knowledge, there are no satisfying mechanisms to improve LTE-V2X Mode 4 performance when aperiodic CAM traffic is considered. This is also evidenced in the comprehensive survey [SURVEY-BAZZI].*
With the aim of putting forth a solution, our approach leverages Machine Learning, that reveals to be a winning choice, as it accurately forecasts when the next CAMs will be generated; it therefore allows to identify the optimal choice of system parameters, i.e., the Resource Reservation Interval (RRI) and the reselection counter, so as to efficiently allocate radio resources. Ultimately, it improves system performance and achieves excellent results. Moreover, the proposed strategy relies on the original LTE-V2X Mode 4 access technique, without requiring any significant modification to the standard-compliant mechanism.
This too, is stated in the revised Introduction.

Reviewer #1 concern #2: "Performance evaluation metrics should be discussed."
Author response: *The performance evaluation metrics that are relevant for the vehicular broadcasting scheme are defined in Section IV. The metrics employed for Machine Learning have been newly introduced in Subsection V-B, page 8.*

Reviewer #1 concern #3: "The contributions should be clearly mentioned (also in the light of the existing works)."
Author response: *We thank the reviewer for his/her valuable comment. We significantly modified the Introduction, to clearly state the contributions of our work. Several examples of existing works were newly added, and a critical comparison against our research was provided.*

Reviewer #1 concern #4: "There are typos and grammatical mistakes in the paper that should be removed and corrected, respectively."
Author response: *Urged by the reviewer's remark, we had the manuscript carefully revised by a professional language editing service. All the typos and grammatical mistakes were corrected.*

[ACCESS-LUSVARGHI] L. Lusvarghi, M.L. Merani, "On the Coexistence of Aperiodic and periodic Traffic in Cellular Vehicle-to-Everything," IEEE Access, vol.8, pp.207076-207088, 2020.

[MOLINA] R. Molina-Masegosa, J. Gozalvez and M. Sepulcre, "Comparison of IEEE 802.11p and LTE-V2X: An Evaluation With Periodic and Aperiodic Messages of Constant and Variable Size," IEEE Access, vol. 8, pp. 121526-121548, 2020.

[SURVEY-BAZZI] A. Bazzi, A. O. Berthet, C. Campolo, B. M. Masini, A. Molinaro and A. Zanella, "On the Design of Sidelink for Cellular V2X: A Literature Review and Outlook for Future," IEEE Access, vol. 9, pp. 97953-97980, 2021.

Reviewer: 2

In this manuscript, the authors have proposed a machine learning-based approach to disseminating aperiodic cooperative awareness messages in V2V communication. The topic is interesting and timely. However, I have some concerns which I am listing below.

Reviewer #2 concern #1: Why there is a need for an ML-based approach in data disseminating in V2V communication is not explained properly. Authors should clearly mention how the heterogeneity of vehicles is going to affect the overall system decision.

Author response:

When broadcasting aperiodic traffic, like CAMs, Machine Learning plays a central role. Its accurate prediction of future CAM inter-arrival times allows the ego-vehicle to reserve resources using the optimal configuration of the Resource Reservation Interval (RRI) and of the reselection counter. This is explained in the last paragraph of Subsection III-B.

It follows that the adoption of Machine Learning minimizes the latency reselections and the unused reservations, which are the main sources of performance degradation when aperiodic traffic is considered. As a matter of fact, latency reselections should be avoided as much as possible, as they ultimately increase the probability of packet collisions. Unused reservations do not allow vehicles to correctly announce their reserved resources, which are therefore sensed as free from neighboring users; in this case too, the probability of packet collision increases. These two effects are discussed in Subsection II-B.

As regards the impact of the heterogeneity of vehicles, the larger the number of vehicles employing the ML-based approach, the better the overall system performance will be. If some vehicles were not to employ the KNN algorithm for the optimal configuration of the RRI and Cresel parameters, latency reselections and unused reservations would inevitably increase; in turn, the probability of packet collisions would increase.

Reviewer #2 concern #2: Authors should clearly mention the existing state-of-the works in this particular area. Along with that, clearly mention what are novel contributions that authors have made in this work. Is introducing the ML approach is the only contribution?

Author response: *As suggested by the reviewer, the revised manuscript clearly mentions the existing state-of-the-art works and the novel contributions we provided.*

Our work leverages Machine Learning for predicting the CAM patterns and it improves the performance of the standard-compliant SSPS mechanism used for selecting and reserving resources. In addition, we propose to include the reselection counter value within the Sidelink Control Information (SCI) and to avoid the creation of the second list, L2, during the list creation phase. These modifications further improve the collision-detection capability of the SSPS mechanism.

Reviewer #2 concern #3: In Section II, What is an ego-vehicle? Further, during list creation, are the vehicles aware of the total number of neighboring vehicles beforehand? How the effect of vehicle movement of its list creation. The authors should clearly state the system model/scenario they have considered for their analysis to improve the readability of the paper.

Author response: *In literature, the "ego-vehicle" identifies the connected vehicle whose behavior is of primary interest. As such, in our work, the term "ego-vehicle" is used to indicate the vehicle that selects and reserves new resources using the SSPS mechanism. The definition of the ego-vehicle was added in Subsection II-A.*

During the list creation phase, the ego-vehicle exploits the Sidelink Control Information (SCI) received from neighboring users to learn which resources have not already been reserved by other vehicles. The list creation phase adheres to its 3GPP specifications provided within the 3GPP standard documents [TS36.213]. Therefore, the ego-vehicle is not required to know the number of neighboring vehicles beforehand.

Moreover, vehicle movement is not affecting the list creation phase. The list creation phase exclusively relies on the SCI received from the neighboring vehicles.

We strived to exhaustively describe the system model and scenario in Section V-A and in the first paragraph of Section V-B. We would greatly appreciate any detailed and explicit comments about the content of these two Sections, to understand what is missing in the description of the setting we investigated.

[TS36.213] 3GPP, "Evolved Universal Terrestrial Radio Access (E-UTRA); Physical Layer Procedures," TS 36.213, V16.6.0, June 2021.

Reviewer #2 concern #4: In resource selection and reservation, from where the values of RRI, P, C_{min}, and C_{max} are considered? Is it defined in standard? If yes, then the authors must mention the source.

Author response: *The values of RRI, P, C_{min} and C_{max} employed in this work are drawn from the 3GPP specifications. In the revised manuscript, we included the references to the standard documents in Subsection II-A.*

Reviewer #2 concern #5: In Section II-C, the authors mentioned that the inter-arrival time between consecutive messages is variable and its duration strongly depends on vehicle dynamics. What do the authors mean by vehicle dynamics?

Author response: *In Subsection II-C, the term "vehicle dynamics" refers to the heading, position, and speed variations of the vehicle generating the Cooperative Awareness Messages (CAMs). In Subsection II-C, we better clarified this point.*

Reviewer #2 concern #6: The correlation between CAM inter-arrival times and vehicle behavior is not easy to understand. Although the authors have shown it in Fig. 3, still it requires further explanation. How the presence of other vehicles is going to affect the vehicle behavior.

Author response: *We acknowledge the reviewer's remark and we revised Subsection II-C to provide a more exhaustive explanation for the correlation between CAM inter-arrival times and vehicle dynamics. The way the presence of other vehicles affects the vehicle behavior is something that cannot be easily predicted: a vehicle may slow down, change lane, overtake, and so forth. In this respect, Machine Learning is particularly useful for predicting how the*

ego-vehicle will react to the presence of other vehicles and how the generated CAM patterns will accordingly vary.

Reviewer #2 concern #7: The strong correlation between CAM inter-arrival times and vehicle dynamics suggests that the adoption of ML can be beneficial to predict the temporal evolution of CAM sequences. Justify the reason behind it properly. In the proposed ML-based approach, what are the input parameters to the model. Does the packet collision parameter taken into consideration?

Author response: *Machine Learning explores the training data to identify correlation patterns between vehicle dynamics and CAM traces. Then, such knowledge is challenged on the test data, where the algorithm forecasts future CAM generation times from the input parameters. This clarification was added in the first paragraph of Subsection III-B.*

The input parameters of the model are:

- *trajectory, current speed and position of the ego-vehicle;*
- *current speed and position of the vehicle immediately preceding the ego-vehicle.*

Such parameters were originally listed in the first paragraph of Subsection III-B. In the revised manuscript, we resorted to explicit items, highlighted by bullets, to better evidence them.

Yes, packet collisions are taken into consideration, both when the original SSPS and the proposed solution are considered, as they affect the overall system performance.

Reviewer #2 concern #8: To show the effectiveness of the proposed algorithm, the authors must compare it with any existing state-of-the-art schemes.

Author response: *The existing state-of-the-art scheme is represented by the legacy SSPS standard mechanism, and we compared our results against it all throughout the paper. As commented in the revised Introduction and state-of-the-art, no specific solutions exist to satisfyingly serve real, aperiodic CAM traffic in C-V2X.*

Reviewer: 3

In this paper, the authors proposed a novel Machine Learning (ML)-based method to distribute aperiodic Cooperative Awareness Messages (CAMs). By k-Nearest Neighbors (KNN) ML algorithm to predict the temporal pattern of CAMs to reduce sub-channels collision and ultimately improve Packet Reception Ratio (PRR). The topic is interesting and meaningful. However, some issues still need to be revised in this paper. Our comments are as follows:

Reviewer #3 concern #1: Some sentences contain grammatical and spelling mistakes. The article needs careful editing by someone with technical English editing expertise paying particular attention to English grammar, spelling, and sentence structure.

Author response: *We thank the reviewer for his/her careful reading of the manuscript. The manuscript has been revised and all the grammatical and spelling mistakes were removed.*

Reviewer #3 concern #2: In the explanation of Figure 4, this article does not clearly state the working principles of RRITX and RRIRX. At the same time, the collision situation of the three different sub-channel selections is not clearly stated. Would you please revise it again?

Author response: *Adhering to the reviewer's suggestion, we revised Subsection III-A to more clearly explain the reservation working principles and the meaning of RRITX and RRIRX. We also re-formulated the explanation of the different potential collisions exemplified in Fig.4.*

Reviewer #3 concern #3: In this paper, the SSPS process improved by the KNN algorithm, which effectively improves the PRR, but lacks the explanation process of the theoretical part, and it is recommended to supplement the theoretical part of the analysis.

Author response: *The reason why the KNN algorithm guarantees an improvement is that:*

1. *it retrieves the trajectory, speed, and position of the ego-vehicle, and also the speed and position of the vehicle preceding the ego-vehicle;*
2. *from these input features, it predicts what behavior the ego-vehicle will have in the very next future.*

As any machine learning technique, it learns from the training set and then, its performance is evaluated on the test set. In this study, the former is made of 70% of the CAM trace dataset, the latter by the remaining 30%. In Section III-B, a reference was added to provide the reader a link to the theoretical basis behind the approach.

Reviewer #3 concern #4: Why use the KNN algorithm to predict RRI and Cresel, but not other ML algorithms to achieve this process? It suggests a comparative test of other algorithms in the simulation section.

Author response: *We kindly point out to the reviewer's attention that KNN achieves excellent results. Its accuracy and macro-F1 metrics are well above 0.9, as Figs. 7(a)-(c) and Fig. 8 highlight. We decided to use KNN because it is fast to train and easy to understand, also for people not familiar with Machine Learning. The results demonstrate that its predictions are extremely precise. We could have used a different, more sophisticated ML algorithm to identify the optimal configuration of RRI and Cresel; yet, this would have only led to incremental improvements.*

Moreover, the aim of our article is to show how to improve the resource allocation process of LTE-V2X Mode 4 via the prediction of CAM inter-arrival times and we demonstrated that even the adoption of a simple ML algorithm achieves the result. We elaborated on this point in the revised manuscript, last paragraph of Subsection V-B.

Reviewer #3 concern #5: The total references number is only 23. More recent studies are encouraged to add into this paper, such as: Latency and Reliability of mmWave Multi-hop V2V Communications under Relay Selections.

Author response: *We thank the reviewer for the suggestion. We extended the literature review reported in the Introduction, including additional references, as well as articles that have been published after our initial submission.*

Reviewer #3 concern #6: 6. In the highway scene, due to the constant speed between the vehicles, the CAM arrival time is not much different. The improved KNN algorithm used in this paper cannot achieve a good result. Comparing the results of the Ground Truth (GT) benchmark and the traditional SSPS process, there is still room for optimization in this process. Can other input features be added to KNN to optimize experimental results? Or can we adopt a new SSPS process in a separate scenario?

Author response: *We do not agree with the reviewer's remark that the improved KNN algorithm cannot achieve a good result in the highway setting.*

In detail, in the highway scenario, the proposed Machine Learning-based algorithm is analyzed considering two different CAM generation models.
In the first scenario, CAMs are generated exploiting the vehicular mobility traces obtained through SUMO simulations. Here, the proposed KNN-based algorithm achieves an impressive performance, very close to the Ground Truth (GT) benchmark levels, as Fig. 16 reveals. No room is left for optimization and it is pointless to consider additional input features.
In the second case, realistic CAM patterns are generated employing the mathematical models presented in [EMP-MODELS]. Unfortunately, such models have no notion of vehicle dynamics: in other words, they do not provide the vehicle trajectory, speed, and in general the input features that the ML forecast needs. Therefore, the performance of the KNN algorithm, or of any alternative ML approach, cannot be assessed. Nonetheless, such CAM traces allow to determine the Ground Truth performance, that is, the maximum theoretical improvement that Machine Learning achieves.

Reviewer #3 concern #7: In the highway scenario, this article does not give a solution on how to improve the SSPS reservation strategy?
Author response: *Again, we kindly dissent from the conclusion of the reviewer. We point out to the reviewer's attention that our article does provide a solution on how to improve the SSPS reservation strategy in any type of scenario, including the highway.*
As mentioned in the response to concern #6, Fig.16 shows that the proposed approach leads to a significant performance improvement. Figs. 17 and 18 also indicate that the maximum theoretical improvement is remarkable. The more accurate the employed ML algorithm will be, the closer the predictive reservation approach will get to the GT benchmark.
We added a comment in Subsection V-B to better clarify this and the previous point.

[EMP-MODELS] R. Molina-Masegosa, M. Sepulcre, J. Gozalvez, F. Berens, and V. Martinez, "Empirical models for the realistic generation of cooperative awareness messages in vehicular networks," IEEE Transactions on Vehicular Technology, vol. 69, no. 5, pp. 5713-5717, May 2020